

Interacting multiple-models, state augmented Particle Filtering for fault diagnostics

Michele Compare, Piero Baraldi, Pietro Turati, Enrico Zio

▶ **To cite this version:**

Michele Compare, Piero Baraldi, Pietro Turati, Enrico Zio. Interacting multiple-models, state augmented Particle Filtering for fault diagnostics. Probabilistic Engineering Mechanics, 2015, 10.1016/j.probengmech.2015.01.001 . hal-01262136

HAL Id: hal-01262136
https://hal.science/hal-01262136

Submitted on 26 Jan 2016

HAL is a multi-disciplinary open access archive for the deposit and dissemination of scientific research documents, whether they are published or not. The documents may come from teaching and research institutions in France or abroad, or from public or private research centers.

L'archive ouverte pluridisciplinaire **HAL**, est destinée au dépôt et à la diffusion de documents scientifiques de niveau recherche, publiés ou non, émanant des établissements d'enseignement et de recherche français ou étrangers, des laboratoires publics ou privés.

Interacting multiple-models, state augmented Particle Filtering for Fault Diagnostics

Michele Compare[1,2], Piero Baraldi[1], Pietro Turati[1], Enrico Zio[1,2,3,*]

[1] Energy Department, Politecnico di Milano, Via Ponzio 34/2, 20133, Milan, Italy.
[2] Aramis S.r.l., Via Viviani 8, Milano, Italy.
[3] Chair on Systems Science and the Energetic Challenge, European Foundation for New Energy-Electricité de France, Ecole Centrale Paris and Supelec, France.
[*] Corresponding author: enrico.zio@polimi.it, enrico.zio@ecp.fr, enrico.zio@supelec.fr

Abstract

Particle Filtering (PF) is a model-based, filtering technique, which has drawn the attention of the Prognostic and Health Management (PHM) community due to its applicability to nonlinear models with non-additive and non-Gaussian noise. When multiple physical models can describe the evolution of the degradation of a component, the PF approach can be based on Multiple Swarms (MS) of particles, each one evolving according to a different model, from which to select the most accurate a posteriori distribution. However, MS are highly computational demanding due to the large number of particles to simulate. In this work, to tackle the problem we have developed a PF approach based on the introduction of an augmented discrete state identifying the physical model describing the component evolution, which allows to detect the occurrence of abnormal conditions and identifying the degradation mechanism causing it. A crack growth degradation problem has been considered to prove the effectiveness of the proposed method in the detection of the crack initiation and the identification of the occurring degradation mechanism. The comparison of the obtained results with that of a literature MS method and of an empirical statistical test has shown that the proposed method provides both an early detection of the crack initiation, and an accurate and early identification of the degradation mechanism. A reduction of the computational cost is also achieved.

Key words: Multi Model Systems, Particle Filtering, Fault Detection and Isolation.

INTRODUCTION

In recent years, the development of relatively affordable on-line monitoring technology has yielded a growing interest in dynamic maintenance paradigms such as Condition-Based Maintenance (CBM) [25]. This is based on tracking the health conditions of the monitored equipment and, on this basis, making maintenance decisions. For this, two fundamental issues are: *i*) *detection*, i.e., the recognition of a deviation from the normal operating conditions; *ii*) *isolation* or *diagnostics*, i.e., the characterization of the abnormal state of the system.

In principle, reliable Fault Detection and Isolation (FDI) allows identifying problems at an early stage, thus performing only strictly necessary maintenance actions, to anticipate failures. This avoids the danger of interrupting operations and possibly introducing malfunctions due to errors of maintenance operators.

The appealing potential of CBM for improving maintenance performance has boosted research and industry efforts in FDI techniques, as witnessed by the considerable amount of related literature (see [5], [12], [22], [23], [24], [45], [46] and [47] for surveys). These techniques may be divided into two main categories: data-driven methods, which resort to field data to build empirical degradation models (e.g., Artificial Neural Network (ANN, [6], [50]), Support Vector Machine (SVM, [20]), Local Gaussian Regression (LGR, [33], [42])), and model-based approaches, which utilize mathematical models to describe the degradation mechanism. In both cases, the detection of a change in the component state and the consequent diagnosis are based on the comparison between the output of the model and the data collected from the operating system.

With regards to the model-based approaches, a number of algorithms have been successfully applied to FDI such as reversible jump Markov Chain Monte Carlo (MCMC, [2], [18], [53]), parity space equations [16] and others techniques surveyed by some FDI literature review works [12], [22], [23]. In particular, a variety of filtering algorithms have been developed to tackle FDI problems, which use discretized differential equations to describe the degradation evolution and stochastic noises to take into account the associated aleatory uncertainty. For example, Kalman Filter (KF) has been adopted to detect incidents on freeways [49] and to set a CBM policy on turbine blades affected by creep [4].

However, KF suffers from a limited applicability due to the stringent hypotheses of model linearity and Gaussian noise, which are often not compatible with practical FDI issues. Thus, some generalizations of KF, such as Extended Kalman Filter (EKF, [35], [36]) and Unscented Kalman Filter (UFK, [27]), have been proposed. Nonetheless, there are still situations where these filtering approaches fail, due to high nonlinearity and for non-Gaussianity.

In this context, Particle Filtering (PF) has proven to be a robust technique [3], [14], for tackling realistic FDI problems [51], [52]. In particular, PF has been adopted for FDI within the Multi-Model (MM) systems framework, where the description of the possible component abnormal evolutions relies on a set of models [28]. In this setting, detection aims at identifying when the component starts to leave the nominal mode, whereas diagnostics consists in selecting the model that best fits its current behavior.

Interesting applications of PF to FDI in MM systems have been proposed in [1] and [10], where multiple swarms of particles are contemporaneously simulated, following all alternative models. FDI is, then, based on Log-Likelihood Ratio (LLR) tests on the recorded measurements to estimate for every swarm of particles the probability of being from the right model. However,

these methods are computationally burdensome and memory demanding, as they require tracing a large number of particles.

Alternatively, an approach based on the augmentation of the state vector with a variable indicating whether the component is in normal or abnormal conditions has been propounded in [29], [38], [44] and [48]. This approach can be considered as a generalization of the Interacting Multiple Model (IMM) [19], [31] algorithm by means of PF. The choice among the possible alternative conditions of the system is then taken based on the marginal distribution of the added variable. This allows the filter to automatically lead the particles to follow the right model, by the recorded measurements which force the state vector to modify the value of the added variable. In particular, such variable is chosen continuous in [29], which proposes an ensemble of Monte Carlo adaptive filters, and uses the LLR tests to make the FDI decision. On the contrary, Boolean variables indicating the component state are used in [38] and [44], where explicit models with associated probabilities of occurrence are assumed to be known, and used to compel the particles to evolve according to the different models. Then, the measurements acquired at the updating steps will favor the particles evolving according to the correct model. A further work discussing the augmentation of the state vector with a discrete variable representing the component state is [48]. However, notice that, this work, as well as that in [38] which investigates the potential of such algorithms, has addressed case studies with only two models, additive Gaussian noise, and abnormal conditions where a sharp and abrupt jump in the measured variables is observed. These conditions are rarely verified in practice, when the fault detection and diagnosis concerns a gradually degrading industrial component [11].

In the context of the Interacting Multiple Model systems based on PF, the novelty of the present work consists in the application of the method to a diagnostic problem, whereas previous applications were focusing on the problem of detecting abnormal conditions [1], [10].

Furthermore, the proposed approach allows treating non additive Gaussian noises and, differently to another work which considers only sharp degradations [48], it can be used also in case of gradually evolving degradation processes. An additional contribution of the paper is the comparison of different techniques such as augmented state PF, the LLR-based approach (e.g., [10]) and an intuitive approach based on statistical hypothesis tests [26]. Finally, the influence of the model parameters such as transition matrix entries and measurement error on the IMM PF diagnostic performance is investigated in order to provide hints on the parameters setting.

For the comparison, a case study is considered regarding a non-linear crack growth in a structure. In particular, the following two settings have been investigated:

1) There are only two models available, one for normal conditions and the other for degradation; hence, in this case the detection and diagnosis coincide. This setting allows us to compare the performance of our approach with that of other works of literature (e.g., [38], [44]).
2) The component behavior is described by three models, the two of the previous setting and one additional model describing a different degradation mechanism leading to a different evolution of the crack growth. This allows evaluating the diagnostic capability of the proposed approach, i.e., its ability of selecting the right degradation mechanism.

The remainder of the paper is organized as follows. In Section 2, a general description of the Multi Model setting is presented, with a focus on the case study considered in this work. In Section 3, basics of Particle Filtering are recalled for completeness. Section 4 summarizes the characteristics of the PF-based techniques proposed in the literature to address FDI in Multi Model systems, and describes the particular FDI technique based on the augmented state vector. In Section 5 the application on a simulated but realistic, case study of crack growth is presented. In Section 6 conclusions are drawn and further developments discussed.

2. MULTI MODEL SYSTEM

A Multi Model system is defined as a system which cannot be described by the same model during its entire life; on the contrary, the description of its evolution requires a set of *M* models, each one capturing different behaviors of the system in different situations or phases. Thus, a set of *M* state equations are proposed to describe the different evolutions, which can be divided into two main classes:

N models describing the component operation in normal conditions $m_{n_1}, \dots, m_{n_N}$:

$$\begin{aligned} m_{n_1}&: \boldsymbol{x}_k = \boldsymbol{f}_{k-1}^{n_1}\left(\boldsymbol{x}_{k-1}, \boldsymbol{\omega}_{k-1}^{n_1}\right) \\ &\dots \\ m_{n_N}&: \boldsymbol{x}_k = \boldsymbol{f}_{k-1}^{n_N}\left(\boldsymbol{x}_{k-1}, \boldsymbol{\omega}_{k-1}^{n_N}\right) \end{aligned} \quad \textbf{(1)}$$

D models describing the operation of the component which is degrading according to one of the possible *D* degradation mechanisms $m_{d_1}, \dots, m_{d_D}$ which it can be subjected to

$$\begin{aligned} m_{d_1}&: \boldsymbol{x}_k = \boldsymbol{f}_{k-1}^{d_1}\left(\boldsymbol{x}_{k-1}, \boldsymbol{\omega}_{k-1}^{d_1}\right) \\ &\dots \\ m_{d_F}&: \boldsymbol{x}_k = \boldsymbol{f}_{k-1}^{d_D}\left(\boldsymbol{x}_{k-1}, \boldsymbol{\omega}_{k-1}^{d_D}\right) \end{aligned} \quad \textbf{(1)}$$

where *N*+*D*=*M*, $\boldsymbol{x_k}$ represents the state vector at time t_k, and $\boldsymbol{\omega}_{k-1}$ is the noise at the previous time step, t_{k-1}, which defines the aleatory uncertainty in the evolution of the process. In this work, we assume that the process noise distribution is known, although in real applications it must be inferred from experimental data or retrieved from expert knowledge. The interested reader may refer to [21] for a particle filtering-based technique that allows the joint estimation of the state vector and the unknown parameters of the noise distributions.

A further assumption is that the state $\boldsymbol{x}_k$ cannot be precisely measured, and the knowledge about its value is affected by uncertainty, represented by the noise $\boldsymbol{\nu}_k$**.** The measurement model:

$$\boldsymbol{y}_k = \boldsymbol{g}_k(\boldsymbol{x}_k, \boldsymbol{v}_k) \quad \textbf{(2)}$$

that links the state $\boldsymbol{x}_k$ to the acquired measurement $\boldsymbol{y}_k$ is supposed to be given.

As example of MM system, in this work, we consider a fatigue crack growth degradation mechanism in a mechanical component (Fig. 1). Crack growth is typically modeled in three phases [7], [13], [17], [43]:

i) *Normal conditions*: crack incubation; it is the short initial phase of the phenomenon, which is connected with plastic strains locally occurring in the most stressed parts of the mechanical component subject to cyclic loads. At this stage, coalescence of dislocations and vacancies, as well as ruptures due to local stresses lead to the formation of sub-microcracks in the slip bands at the boundaries of blocks, grains and twins. From the practical point of view, in this phase the crack length is modeled by a constant which is set to zero, being its exact value not measurable by traditional measurement instrumentation when the component is in this phase.

ii) *Degradation mechanism 1*: crack initiation; it is characterized by the growth and coalescence of the sub-microcracks, which transform into micro-cracks; these start increasing under the cyclic loads, and form macro-cracks, which are typically detectable by measurement instrumentation. This process gives rise to the third phase. The model describing this second phase is linear in time [8]. This second phase can also be considered as the "threshold region" among the fatigue crack regions described by NASGRO equations [13], [43].

iii) *Degradation mechanism 2*: crack rapid-propagation; the crack grows under cyclic loads, up to a critical threshold. A number of models have been proposed to describe this latter phase, such as the Paris-Erdogan exponential law [40] here considered. According to the NASGRO model, this phase corresponds to the linear region (in logarithmic scale), also called Paris region [13], [43].

The measurements recorded to monitor the degradation process are affected by errors, especially during the second phase or when the crack cannot be directly measured due to its position. In this

setting, detection consists in the identification of the deviation from the first phase, while diagnostics consists in determining whether the degradation mechanism is linear (i.e., the second phase) or exponential (i.e., the third phase).

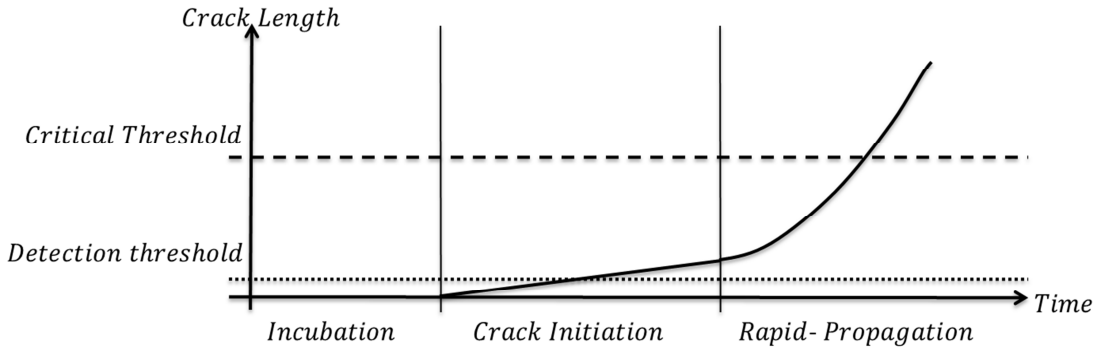


Fig. 1 Schematic approximation of the crack propagation model.

3. PARTICLE FILTERING

Particle Filtering (PF) is a sequential Monte-Carlo method, which is made up of two subsequent steps: prediction and updating. At time t_{k-1}, the prediction of the equipment state $\boldsymbol{x}_k$ at the next time instant t_k, is performed by considering a set of N_S weighted particles, which evolve independently on each other, according to the given probabilistic degradation model (i.e., one out of those in Eqs. **(1)**). The underlying idea is that such group of weighted random samples provides an empirical discrete approximation of the true Probability Density Function (pdf) $p(\boldsymbol{x}_k|\boldsymbol{Y}_{k-1})$ of the system state $\boldsymbol{x}_k$ conditional on the available measurements until time t_{k-1}, where $\boldsymbol{Y}_{k-1} = \{y_0, \dots, y_{k-1}\}$. When a new measurement $\boldsymbol{y}_k$ is acquired, it is used to update the proposed pdf in a Bayesian perspective, by adjusting the weights of the particles on the basis of their likelihood of being the correct value of the system state. For practical purposes, PF works as if the n-th particle, $n = 1, 2, \dots N_S$ were the real system state; then, the smaller the probability of observing the last collected measurement, the larger the reduction in the particle weight. On the

contrary, when the acquired measurement matches well with the particle state, then its importance is increased. Such updating step of the particle weights is driven by the probability distribution $p(\boldsymbol{y_k}|\boldsymbol{x_k})$ (which is derived from Eq. **(2)**) of observing the measurement $\boldsymbol{y_k}$ given the true degradation state $\boldsymbol{x_k}$, and provides the distribution $p(\boldsymbol{x_k}|\boldsymbol{Y_k})$.

The PF scheme used in this work is the Sequential Importance Resampling (SIR, [3], [14]), which builds a new population of particles by sampling with replacement from the set of particles $\{\boldsymbol{x}_k^1, \dots, \boldsymbol{x}_k^{N_s}\}$; the chance of a particle being sampled is proportional to its weight w_k^n. The final weight assigned to the particles of such new set is $\frac{1}{N_S}$. The SIR algorithm allows avoiding the degeneracy phenomenon (i.e., after few iterations, all but few particles would have negligible weights), which is typical of the standard version of PF (i.e., Sequential Importance Sampling, SIS). Finally, the updated particle distribution is used to perform the successive prediction step up to the next measurement (for further theoretical details see [3], [14], [15] and [32]).

4. PARTICLE FILTER FOR DETECTION OF ABNORMAL CONDITIONS AND DIAGNOSIS IN MULTI MODEL SYSTEMS.

PF has been already applied for FDI in MM systems. For example, in [28], PF is used to simultaneously run swarms of particles evolving according to every model available (Fig. 2). Then, a residuals analysis or a Log-Likelihood Ratio (LLR) test is performed to identify the swarm that best matches with the observed measurements and, thus, the corresponding model. For example, Fig. 2 shows the case in which three different swarms are traced by PF, according to three available models m_n, m_{d1} and m_{d2}. Model m_n is the best model to represent the system evolution in its first phase, being very good the matching of the corresponding particle swarm and the measurements acquired at time instants T_1, T_2, T_3; on the contrary, at time T_5 the model which best fits the measurements becomes m_{d2}.

Enhancements of this approach have been proposed in [1] and [10]. In the former work, a new way to estimate the likelihood function is introduced to extend the applicability of the method to more complex particle distributions. In the latter, a swarm of particles for every possible evolving model is created at every time step, and traced to detect the occurrence of abnormal conditions at any subsequent time instant. For example, Fig. 3 shows that two new swarms are created at every measurement step, which evolve according to models m_{d1} and m_{d2}, alternative to the nominal conditions model m_n. The presence of diverse swarms increases the promptness in detecting the change in the behavior of the system, which is again established by LLR tests. On the other side, this advantage is counterbalanced by the onerous computational time due to the large number of particles to be simultaneously traced. To partially overcome this problem, the authors in [10] have proposed to consider an observation window, at the end of which the swarms are no longer traced. Obviously, the width of such time window needs to be set large enough to allow the LLR to robustly detect model changes. Then, this approach is not effective when the models need a long transition time to significantly diverge, as this would require fixing wide observation windows. Furthermore, the number of particles to be drawn increases with the number of system models.

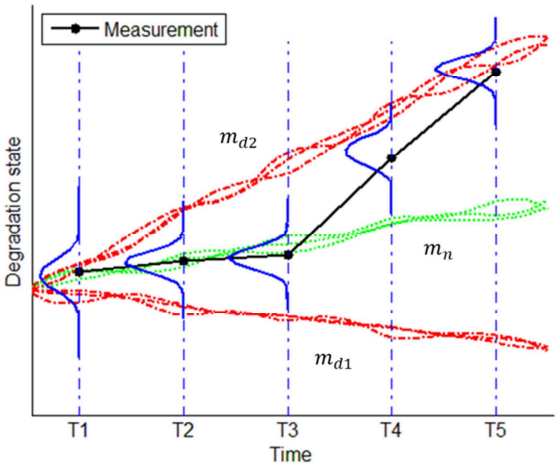


Fig. 2 Parallel swarms of particles evolving according to the available models. At every T_k, particle weights are updated driven by $p(y_k|x_k)$.

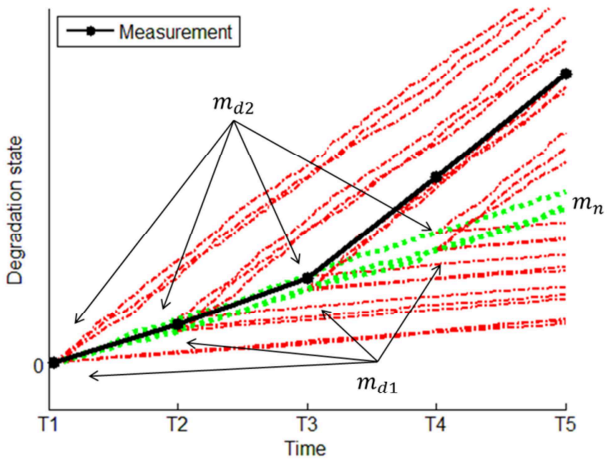


Fig. 3 At every time step, new swarms of particles start according to the alternative models.

A different way to tackle the MM problems is that of augmenting the state vector with a new discrete variable, which represents the evolution model of the system. That is, the state vector becomes $\dot{\boldsymbol{x}}_k = [\boldsymbol{x_k}\ \theta_k]^T$, and the degradation models in Eq. **(1)** are embedded in the model:

$$\dot{\boldsymbol{x}}_k = f'\left(\dot{\boldsymbol{x}}_k, \boldsymbol{\omega}_{k-1,\theta_{k-1}}\right) = f'\left(\boldsymbol{x_{k-1}}, \theta_{k-1}, \boldsymbol{\omega}_{k-1,\theta_{k-1}}\right) \quad \textbf{(3)}$$

where f' encodes also the probabilistic model governing the transitions among the different possible models, which is a first-order Markov chain [48].

This setting requires modifications to the PF algorithm. In details, the PF prediction step has to give due account to the possible alternative models according to which the particles are simulated:

$$p(\grave{\boldsymbol{x}}_k|\,\boldsymbol{Y}_{k-1}) = \int p(\grave{\boldsymbol{x}}_k|\grave{\boldsymbol{x}}_{k-1})p(\grave{\boldsymbol{x}}_{k-1}|\,\boldsymbol{Y}_{k-1})d\grave{\boldsymbol{x}}_{k-1} =$$

$$\int \sum_{\theta_{k-1}} p(\boldsymbol{x}_k, \theta_k|\boldsymbol{x}_{k-1}, \theta_{k-1})p(\boldsymbol{x}_{k-1}, \theta_{k-1}|\,\boldsymbol{Y}_{k-1})\, d\boldsymbol{x}_{k-1} = \tag{4}$$

$$= \int \sum_{\theta_{k-1}} p(\boldsymbol{x}_k\,|\boldsymbol{x}_{k-1}, \theta_k)p(\theta_k\,|\,\theta_{k-1})p(\boldsymbol{x}_{k-1}, \theta_{k-1}|\,\boldsymbol{Y}_{k-1})d\boldsymbol{x}_{k-1}$$

In the last equation, it is assumed that the transition probabilities $p(\theta_k\,|\,\theta_{k-1})$ do not depend on the current degradation state $\boldsymbol{x}_{k-1}$, whereas the prediction of the state $\boldsymbol{x}_k$ depends on the added variable θ_k, whose value is sampled at the current time instant t_{k-1}.

The successive updating step at time t_k concerns the evaluation of the weights w_k^n of the particles $\grave{\boldsymbol{x}}_k^n$, $n = 1, \dots, N_s$, given the new measurement $\boldsymbol{y}_k$. The particles and their weights approximate the posterior distribution as a weighted sum of Dirac distributions $\delta(\grave{\boldsymbol{x}}_k - \grave{\boldsymbol{x}}_k^n)$, centered on the particle positions:

$$p(\grave{\boldsymbol{x}}_k|\,\boldsymbol{Y}_k) = \frac{p(\boldsymbol{y}_k|\grave{\boldsymbol{x}}_k)p(\grave{\boldsymbol{x}}_k|\boldsymbol{Y}_{k-1})}{p(\boldsymbol{y}_k|\boldsymbol{Y}_{k-1})} \approx \sum_{n=1}^{N_S} w_k^n \cdot \delta(\grave{\boldsymbol{x}}_k - \grave{\boldsymbol{x}}_k^n) \tag{5}$$

The non-normalized weights are updated as follows:

$$\widetilde{w}_k^n = w_{k-1}^n \cdot p(\boldsymbol{y}_k|\grave{\boldsymbol{x}}_k^n) = \frac{1}{N_S} \cdot p(\boldsymbol{y}_k|\boldsymbol{x}_k^n), \tag{6}$$

where the right term is justified by the fact that the likelihood depends on the state $\boldsymbol{x}_k$, only, and the resampling step at t_{k-1} has led to $w_{k-1}^n = \frac{1}{N_S}, n = 1, \dots, N_S$. Then, a resampling step is used to sample a new population $\grave{\boldsymbol{x}}_k^{n_{new}}$ of N_s particles from the already available weighted swarm of particles: each new particle is sampled with a probability proportional to $\widetilde{w}_k^n$ and has an associated new weight, $w_k^n = \frac{1}{N_S}$: thus, the higher the weight $\widetilde{w}_k^n$ the larger will be the number of resampling particles equal to $\grave{\boldsymbol{x}}_k^n$.

Nonetheless, favoring the particles positioned in the neighborhood of the measurement, $\boldsymbol{y}_k$, leads to the selection of the particles with the most likely value of θ_k.

For the sake of clarity, the transition probabilities $p(\theta_k \mid \theta_{k-1})$ in Eq. **(4)** can be arranged in the matrix:

$$A_{trans} = \begin{bmatrix} A_{11} & A_{12} & \dots & A_{1M} \\ A_{21} & A_{22} & \dots & A_{2M} \\ \dots & \dots & \dots & \dots \\ A_{M1} & A_{M2} & \dots & A_{MM} \end{bmatrix} : A_{ij} \geq 0, \forall\, i,j = 1,2,\dots M \qquad \textbf{(7)}$$

where the i-th element of the j-th column represents the probability that a particle which has been simulated according to model i, will be simulated at the next step according to model j.

For example, in the case in which there are M=2 alternative models, model 1 refers to the normal state (N=1), whereas model 2 to the degradation state (D=1). Then, A_{11} is the probability that a particle which at the previous step has been simulated according to model 1, will be simulated again according to the same model 1, whereas A_{12} is the opposite case, i.e., the same particle will change its stochastic behavior. Fig. 4 gives a pictorial view of this dynamics.

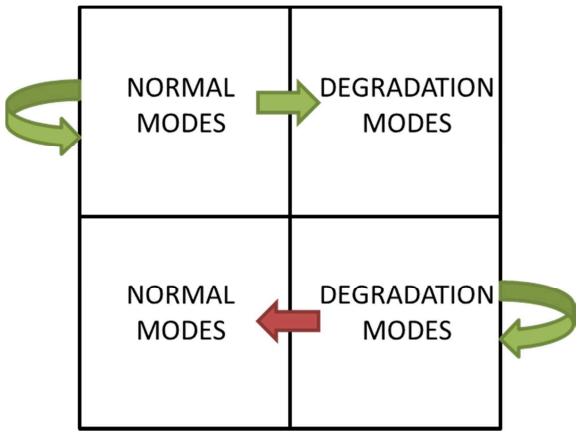


Fig. 4 Possible transitions among the operational models of the system.

Notice that the transition from model j to model i, $j > i$, is physically meaningless when it is not possible that a system spontaneously recovers by itself. However, in the considered setting a

positive value is always given to the corresponding probabilities. In fact, if these were set to zero, the system would be biased to follow the degradation models, especially in case of outlier measurement values, as the trajectories of those particles that are erroneously following a degradation model could no longer be corrected.

For the sake of clarity, an example of the dynamic evolution of the particles when the measurements are collected from the normal operating system is given in Fig. 5. At time t_0, some particles change their reference model according to A_{trans}. In particular, some particles experience a change of the variable θ_k from θ_N to θ_D. These particles are strongly unfavored at the updating step, being the acquired measurement far from their states. Thus, among the particles with state parameter θ_D, only few particles (one in Fig. 5) are resampled and still follow the wrong model at the next time step, whereas the others are reset to the starting point. The behavior of the augmented MM PF in the opposite case, i.e., when measurements are acquired from a degrading component, is shown in Fig. 6. There, during the updating and resampling steps, the number of particles having θ_D as augmented state increases. Hence, the acquired measurements promote the particles associated to the correct model, i.e., those labeled with the correct value θ_D of the added variable, which are closer to the measured degradation value. This allows the particles to auto-adapt their trajectories to the real evolution of the component and, thus, selecting the correct model.

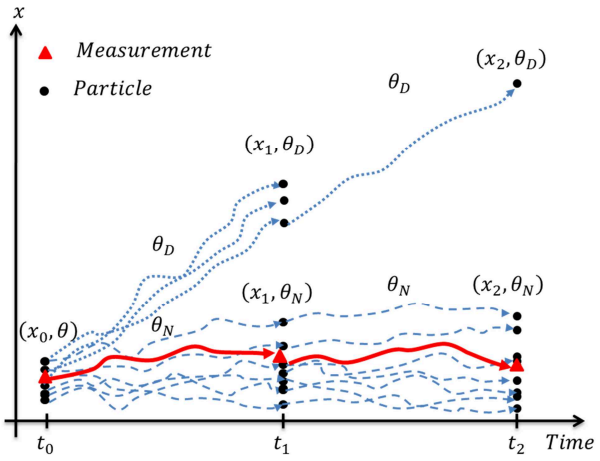


Fig. 5 Evolution of a system as long as measurements support the normal model.

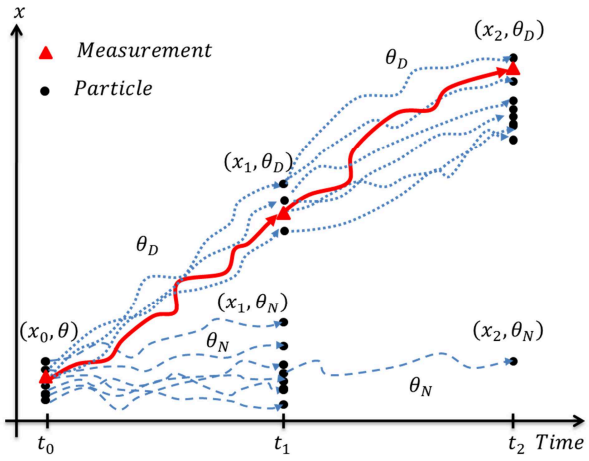


Fig. 6 Evolution of the system and correlated swap in the model parameter, due to measurements supporting the degradation model.

In this framework, the probability associated to each operational model can be estimated at every time step by marginalizing the updated particle distribution:

$$\mu_k^i = p(\theta_k = m_i | \boldsymbol{Y}_k) = \int p(\boldsymbol{x}_k, \theta_k | \boldsymbol{Y}_k)\, d\boldsymbol{x}_k \tag{8}$$

From the practical point of view, this is equivalent to summing the updated probability masses of the particles evolved according to model m_i. On this basis, the probability of the system being in normal conditions is given by:

$$\mu_k^{norm} = p(\theta_k \in M_{norm} | \boldsymbol{Y}_k) = \sum_{i=1}^{N} p\left(\theta_k = m_{n_i} | \boldsymbol{Y}_k\right) \tag{9}$$

where $M_{norm} = \{m_{n1}, \dots, m_{n_N}\}$ is the set of all the models describing normal conditions. The detection of abnormal conditions can be based on the comparison of μ_k^{norm} with a proper threshold value μ_T (e.g., μ_T=0.05). That is, if $\mu_k^{norm} < \mu_T$, then it is reasonable to conclude that the system is in a degradation state.

With regards to the diagnostic task, the Maximum A Posteriori (MAP) criterion can be used [48]. In details, the model, say *H*, corresponding to the maximum value of μ_k^i is selected among all the possible M models describing the component behavior:

$$\mu_k^H = \max_{i=1,\dots,M} \mu_k^i \quad \textbf{(10)}$$

If model *H* is different from that currently used to describe the system evolution, and μ_k^H is considerably larger than the values μ_k^i associated to all the other models, then a change in the system state is diagnosed. In this respect, to make more robust decisions and reduce the number of false alarms, i.e. wrong identifications of the occurrence of a degradation phase, one can require confirmation by requiring that the criterion be fulfilled for a number of consecutive time steps.

Finally notice that for the sake of generality, in the model considered in Eq. **(3)** the stochastic noise ω_{k,θ_k} depends not only on time, but also on the value of θ_k, i.e., on the operating model; this allows giving due account to the different variability of the alternative models. For example, if the amount of information about the normal operating conditions is larger than for the degradation mechanisms, then the corresponding noise ω_{θ_i}, $\theta_i \in M_{degradation} = \{m_{d1}, \dots, m_{d_D}\}$ is expected to have higher variability than ω_{θ_j}, $\theta_j \in M_{norm} = \{m_{n1}, \dots, m_{n_N}\}$.

For clarity, the pseudo code of the algorithm is reported in Table 1.

Time $= k - 1$

1. Prediction step: it estimates $p(\dot{\boldsymbol{x}}_k | \boldsymbol{Y}_{k-1})$ using (4).

   For $n = 1, \dots, N_S$

   Sample θ_k^n from $p(\theta_k | \theta_{k-1}^n)$,

   Sample $\boldsymbol{x}_k^n$ from $p(\boldsymbol{x}_k | \boldsymbol{x}_{k-1}^n, \theta_k^n)$

   End

2. Updating step: when the new measurement $\boldsymbol{y}_k$ becomes available, it is used to update $p(\boldsymbol{x}_k | \boldsymbol{x}_{k-1}^n, \theta_k^n)$ by applying (5) and (6).

   For $n = 1, \dots, N_S$

   Evaluate the non-normalized weights $\tilde{w}_k^n = \frac{1}{N_S} \cdot p(\boldsymbol{y}_k | \boldsymbol{x}_k^n)$,

   End

3. Resampling step: A new approximation of $p(\dot{\boldsymbol{x}}_k | \boldsymbol{Y}_k)$ based on a swarm of particles having equal weights $\frac{1}{N_S}$ is found.

   For $n_{new} = 1, \dots, N_S$

   Sample $\dot{\boldsymbol{x}}_k^{n-new}$ from a $Multinomial\left(\frac{\tilde{w}_k^1}{\sum_{n=1}^{N_S} \tilde{w}_k^n}, \dots, \frac{\tilde{w}_k^{N_S}}{\sum_{n=1}^{N_S} \tilde{w}_k^n}\right)$ distribution whose categories are the previous particles $\{\dot{\boldsymbol{x}}_k^1, \dots, \dot{\boldsymbol{x}}_k^{N_S}\}$,

   End

4. Diagnostic step: it identifies the most likely model, μ_k^H, by marginalizing $p(\dot{\boldsymbol{x}}_k | \boldsymbol{Y}_k)$ on the augmented state θ_k. This is done by computing:

   $p(\theta_k^i | \boldsymbol{Y}_k) = \mu_k^i = \frac{\#(\theta_k^{n-new} = m_i)}{N_S}, i = 1, \dots, M$

   and identifying the most likely model:

   $\mu_k^H = \max_{i=1,\dots,M} \mu_k^i$,

Table 1 Sketch of the algorithm for PF in the IMM system for fault detection and diagnostics.

5. CASE STUDY – DETECTION & ISOLATION

We consider the crack growth in a component subject to fatigue. Given the lack of an experimental setup, crack growths are simulated using literature models [9], [37], [41]. The FDI

performance of the proposed method (which is here labeled as IMM, according to the terminology used in [19] and [48]) is evaluated in two different settings:

1) There are two models available, one for normal conditions and the other for degradation; hence, the detection and diagnosis tasks coincide. This is the same setting of other works of literature (e.g., [38], [44]). In this case, the performance of the IMM method is compared with that of the MS LLR-based method proposed in [10] and that of an intuitive, statistical test (here referred to as ST).
2) There are three models available, one for normal conditions and two for two different degradation mechanisms of the component. This case is considered in order to evaluate the diagnostic capability of the proposed approach in identifying which degradation mechanism is occurring.

5.1 TWO-MODEL SETTING

5.1.1 Model description

The crack growth evolution is here described as a two phase process:

1) Normal conditions: during the crack incubation phase, we assume that the crack is not propagating. In practice, since in this phase the crack length is very small and, from a practical point of view we are not interested in estimating its exact value, we do not model the microscopic phenomena occurring in the component. Thus, the mathematical model used to describe the time evolution of the crack lengths, $x(t)$, is:

$$m_n : x_k = \begin{cases} x_{k-1} & if\ x_{k-1} < \epsilon \\ \sim Unif\big([0, \epsilon)\big) & otherwise \end{cases} \quad \textbf{(11a)}$$

where the parameter ϵ is a very small constant value, which represents the maximum size of possible microcrack states. In our case ϵ is set to $0.05 \cdot mc$, with *mc* indicating the resolution of the measurement instrument. Notice that although equation (11a), which

models the crack lengths at time t_k as a function of the crack lengths at time t_{k-1}, does not strictly constitute a first order Markov process since it provides a deterministic model of the crack evolution, it will be used in a particle filtering framework in presence of noisy measurements. Eq. (11b) is used to set x_k equal to a random value between $[0, \epsilon)$, when, after a model transition, the crack returns to the normal condition.

2) Degradation: in this phase, the crack propagation is modeled by the Paris-Erdogan model [40]:

$$m_d : x_k = \begin{cases} x_{k-1} + C \cdot e^{\omega_k} \left(\beta \cdot \sqrt{x_{k-1}}\right)^n & if\ x_{k-1} > \epsilon \\ \epsilon & otherwise \end{cases} \quad \textbf{(12)}$$

With respect to the setting of the model parameters, their values are derived from [9], [37], [41] where a detailed description of their physical meaning is provided together with an explanation of their adimensionality. In particular, $C = 0.005$ and $n = 1.3$ are parameters related to the component material, and are determined by experimental tests; $\beta = 1$ is a constant related to the characteristics of the load and the position of the crack. According to [9], [37] and [41], a non-additive process noise $\omega_k \sim N(0,1)$ is used to describe the uncertainty in the growth speed. For a detailed discussion of the randomization of the Paris–Erdogan model and its justification on the basis of empirical data, the interested reader may refer to [30]. Here, we just point out that this representation of the process noise implies that on average e^{ω_k} is greater than 1 and, thus, the degradation process is accelerated with respect to that which would be obtained by the same model without process noise. This fact has been properly considered when model parameters have been set [9], [37], [41]. Finally, the discretized time unit is here assumed to be expressed in arbitrary units of time.

The measurement model is:

$$y_k = \begin{cases} v_k & , x_k \leq mc \\ x_k + v_k & , x_k > mc \end{cases} \quad \textbf{(13)}$$

where $v_k \sim N(0, \sigma_{v\,rif})$ is an additive Gaussian measurement error with standard deviation $\sigma_{v\,rif} = 0.5$. This representation of the measurement error is typically used in case of instrumentation well calibrated but subject to electric noise. Furthermore, the measurement instrument is assumed to have a resolution $mc = 0.4$, which means that it is not capable of observing cracks with length $x_k \leq mc$.

Notice that when the crack length is less than the measurament resolution, it cannot be estimated using the PF approach since the measurament is independent from the crack lenght. Nevertheless, since it is not possible to know a priori if a measurement is pure white noise or it is driven by the crack length, during the updating step we always use the equation below in (13) to drive the PF.

Fig. 7 shows a possible crack evolution and the associated measurements, whereas Fig. 8 shows 100 simulated crack evolutions without the measurement error. These curves highlight the uncertainty associated to the crack growth process.

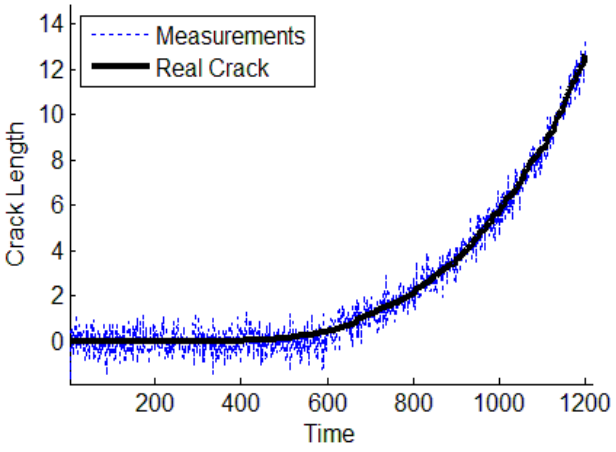


Fig. 7 Crack growth simulation of a crack started at $t_k = 400$h.

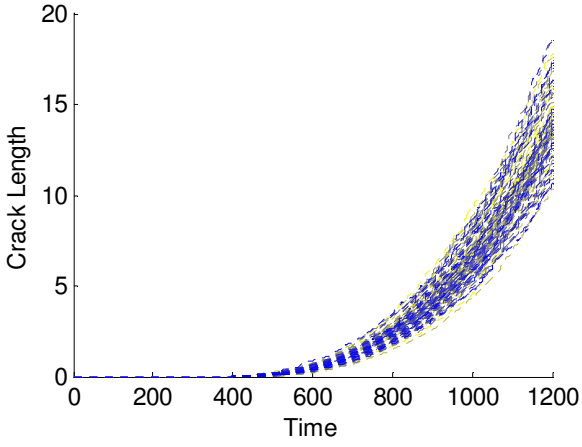


Fig. 8 Simulation of 100 crack evolutions

5.1.2 Performance evaluations

- Interacting Multiple Model (IMM)

The transition probability matrix for the model parameter θ_k has been arbitrarily chosen as:

$$A_{trans} = \begin{bmatrix} 0.99 & 0.01 \\ 0.01 & 0.99 \end{bmatrix} \quad \textbf{(14)}$$

The probabilities that the particles change the reference model are set, at a first attempt, to very small values, i.e., $A_{12} = A_{21} = 0.01$, for the following reasons:

a) with regards to A_{12} (transition probability from the incubation to the crack propagation phase), the larger its value, the larger the expected number of particles that start evolving according to the degradation model. For example, if the number of particles is set to $N_{S_{IMM}} = 100$, then, on average, at every time step a particle of the swarm is forced to swap model. This entails that when a measurement is acquired from a system in normal conditions (crack incubation phase), the particles with augmented variable set to θ_D are unlikely to be resampled, and the swarm continues evolving in the correct way. On the contrary, if the probability A_{12} were set to a larger value, e.g., 0.2, there would be 20 particles evolving according to the degradation model. This means that the probability of having a particle resampled from this set becomes large, especially in the presence of an outlier measurement. Hence, large values of A_{12} make the filter too much sensitive to the measurement noise, with consequent increase in the probability of having false alarms.

b) With regards to A_{21} (transition probability from the crack propagation to the incubation phase), it should be borne in mind that the speed of growth of the modeled crack, and thus of the particles evolving according to such model, is small. Furthermore, when the particles that are correctly associated to the variable $\theta_{k-1} = \theta_D$ are forced to change the prediction model (i.e., $\theta_k = \theta_N$), their crack lengths are reset to 0. Thus, they need a long time to re-catch the real crack

length. These considerations entail that if the transitions $\theta_D \rightarrow \theta_N$ occur too frequently (high value of A_{21}), then the distribution of the particles turns out to be non-conservatively biased, with consequent delay in crack detection. Typically, the smaller the speed of growth, the smaller should be A_{21}, as it will be confirmed by the analysis below.

Fig. 9 shows the good filtering capability of the proposed IMM method, which can be seen from the closeness of the filtered and simulated crack growth evolutions.

Recall that in the present case study there are only 2 models available: then, the detection of abnormal conditions coincides with diagnostics, and the marginalized distribution in Eq. **(8)** is split only between two discrete states. Hence, the alarm threshold can be set at a large value (e.g., $\mu_T = 0.985$) to guarantee a low probability of false alarms while not compromising the prompt detection. Fig. 10 shows an example of how the probability of being in a degradation model has a steep increment and crosses the alarm threshold μ_T (dashed horizontal line) few time steps after the time instant in which the real crack has reached the mc threshold (dashed vertical line). In this respect, notice that, as mentioned above, when the crack length is smaller than mc, it cannot be detected (Eq. **(13)**). Then, the optimal time $T_{optimal\ detection}$ to detect the crack is necessarily larger than the time instant at which the second phase of the crack growth process starts (bold continuous vertical line).

Notice also that the spike highlighted in Fig. 10 is due to an outlier measurement, which could be confused with a measurement acquired from a system in normal conditions (with no crack). Nevertheless, the method shows its robustness, being the spike not capable to force a change in the model identification.

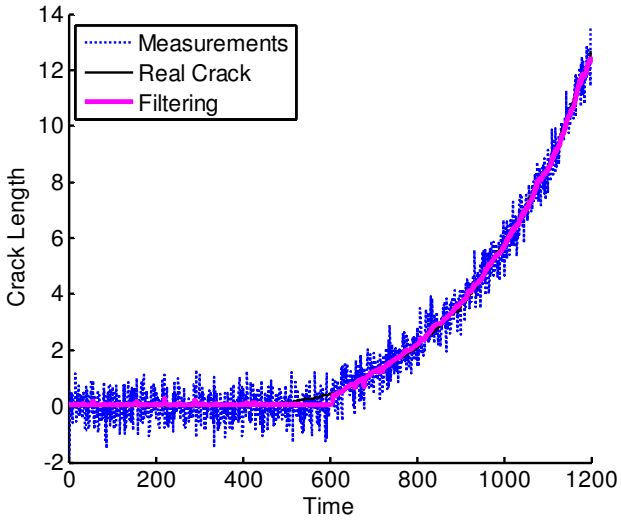


Fig. 9 Filtering crack length via IMM method.

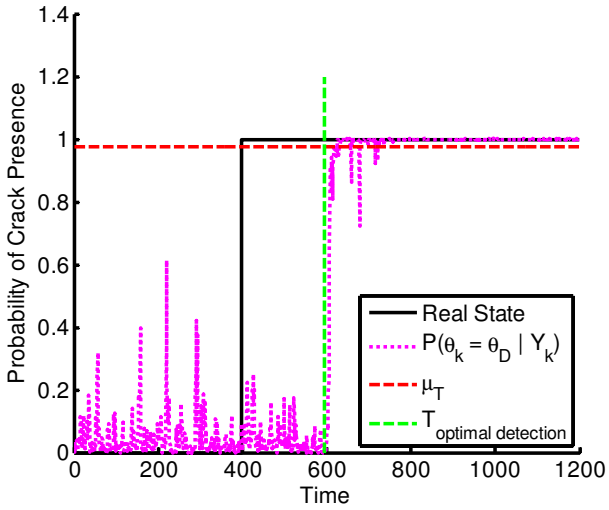


Fig. 10 Marginal posterior probability associated to the degradation model.

- Multiple Swarms (MS).

In this paragraph, the method proposed in [10] is applied to the two-model case study considered. The number of particles for each swarm is set to $N_{S_{MS}} = 25$; this guarantees that each swarm provides a robust statistics in support of the LLR test. The observation time window is set to $w = 100$, which is large enough to take into account the slow initial speed of growth. The minimum number of successive swarms that must identify abnormal conditions in order to trigger an alarm, is set to $n = 5$. This reduces the number of possible false alarms induced by outlier measurement values.

Fig. 11 shows an example of crack evolution, with the filtered state estimated by the n out of w swarms that give the detection alarm. There is a very good matching between the real crack evolution and the mean value of the new swarms within the window of $[\sim 560, \sim 660]$ units of time. In particular, according to the MS approach, the extent of such matching between the measurements and the particle distribution is evaluated by a function $g(LLR)$ (details about this

function can be found in [10], [28]): roughly speaking the higher its value, the larger the likelihood that the measurements come from the abnormal model.

Fig. 12 reports the evolution of function g corresponding to the evolution in Fig. 11. Notice that there is a sharp increment in $g(LLR)$ when the 5 swarms start evolving very close to the real crack.

The detection alarm is triggered when $g(LLR)$ crosses the threshold value λ, which is here set to 8. In this respect, to avoid false alarms λ must be such that when the system evolves according to the normal model, possible consecutive measures larger than mc, which entail large values of $g(LLR)$, do not cause a change in the model; on the other side, setting λ to very large values leads to a delay in detection. Thus, $\lambda = 8$ is a compromise value between these two conflicting needs.

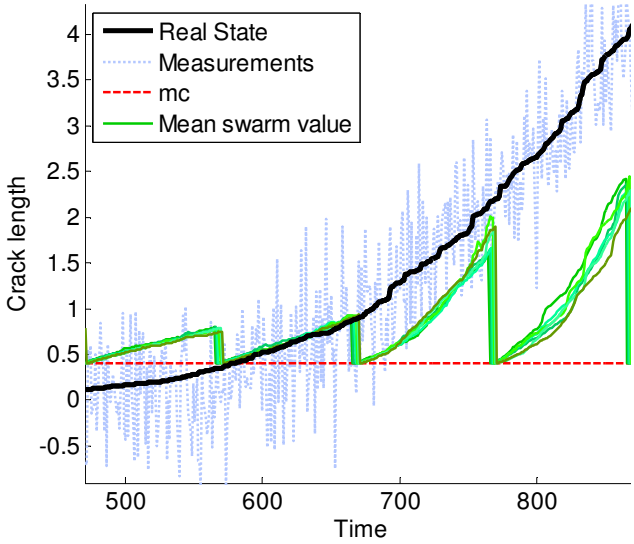


Fig. 11 Filtering crack length for the 5 swarms of particles triggering alarm.

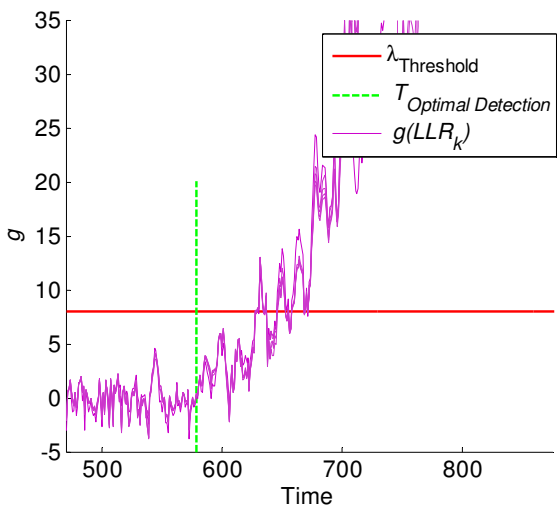


Fig. 12 Function g of the LLR used to set the alarm conditions.

- Sequential Statistic Test (ST)

The detection methods discussed above are compared with an intuitive approach based on a statistical hypothesis test. In details, the test performed is a Z-test for mean with known standard

deviation [26], [39], since the standard deviation of $v_k \sim N(0, \sigma_{v\,rif})$ is assumed to be known. The null hypothesis, H_0, is that the mean value of the measurements is $\mu_y = 0$, whereas the alternative hypothesis, H_1, is that $\mu_y \geq 0$. This entails that H_0 is refused in favor of H_1, when there is the evidence of the crack presence.

To increase the robustness of the method, the alarm is given when H_0 is refused for an established number $seq_{ST} = 4$ of consecutive observations. Thus, if the I type error of each independent test is set to $\alpha_I = 0.1$, the null hypothesis is refused according to a I type error $\alpha_{ST} = {\alpha_I}^{seq_{ST}} = 10^{-4}$. In this respect, notice that if H_0 is true, then the observations are independent and identically distributed random variables.

5.1.3 Performance Indicators

To assess the performance of the different approaches, 100 cracks have been simulated and used for evaluating the following three performance indicators:

1) *Detection Time Delay* [54], i.e., $DTD = T_{detection} - T_{optimal\,detection}$, where $T_{detection}$ is the time at which the marginalized probability μ_k^D of being in state θ_D (crack propagation phase) exceeds the threshold μ_T and $T_{optimal\,detection} = \min_k\{\, k : x_k > mc \,\}$ indicates the time instant at which the crack has reached the mc threshold. DTD is an indicator of the promptness of the method in detecting the change in the model.
2) *Crack Length*, i.e., $CL = \frac{x_{T_{detection}}}{mc}$ which gives an information about the length of the crack at the detection compared to *mc*, i.e. the minimum length value at which the crack could be detected. Values of this indicator close to 1 indicate an accurate detection.
3) *Percentage of False Alarms*, i.e., the number of alarms given when the crack is in the incubation phase (normal conditions), over the number of simulated crack growth processes. It is a widely used index for the robustness of the method.

Notice that false alarms are of primary importance in condition monitoring, since unnecessary stops of a plant for maintenance operation are typically very expensive. In our case study, the 'set points' of the parameters of the considered detection techniques have been set such that the number of false alarms is around an acceptability level of 5%; this is supposed to be the best initial setting to allow a comparison between the three methods.

Table 2 reports the average of the distributions of the three performance indicators in the 100 simulated crack growth trials. From this Table, it appears that the two filtering methods IMM and MS have better performances than ST, being the mean values of the corresponding indicators by far smaller than those of ST. To compare the results of the two filtering methods, we use the one-tail non-parametric Kolmogorov-Smirnov (K-S) test, which allows to test if the cumulative density functions of DTD and of CL provided by IMM are larger than the corresponding ones provided by MS. That is, K-S test checks if the values of DTD and CL provided by IMM are smaller than those provided by MS. The p-values obtained from the K-S tests are 0.0091 and 0.0362, respectively: this confirms the early detection of the IMM method. Also, it must be kept in mind that IMM has a lower computational cost than MS, since it needs to run $N_{S_{IMM}} = 100$ particles instead of $N_{S_{MSTotal}} = N_{S_{MS}} \cdot w = 25 \cdot 100 = 2500$ particles simultaneously simulated in the MS approach. Table 3 reports the computational time required for filtering the evolution of one simulated crack growth in seconds, on a HP Pavilion dv3 Notebook PC.

Notice also that IMM commits less False Alarms than MS (Table 2).

	ST	**IMM**	**MS**
DTD	44.3	19.8	22.1
CL	1.61	1.25	1.28
False Alarms	6%	3%	6%

Table 2 Average Detection Time Delay, Crack Length and Percentage of False Alarms evaluated on a sample of 100 simulated cracks, for the three methods.

	IMM	MS
Computational Time (s)	1.7	32

Table 3 Computational time for filtering crack growth according to the two PF methods analyzed.

The choice of setting the number of particles $N_{S_{IMM}}$=100 has been driven by the authors' experience. The results here obtained show that 100 particles provide a good compromise between the need of reducing the computational efforts and that of obtaining a satisfactory diagnostic performance. In applications requiring higher diagnostic performances, more particles should be employed at the expenses of additional computational time. A sensitivity analysis to investigate how and to which extent this parameter affects the performance is out of the scope of the present work.

Finally, sensitivity analyses have been performed in order to evaluate the dependences of the performance from the transition probabilities and from the variability of the measurement noise.

In details, the sensitivity of the proposed methods to the transition probability matrix has been investigated by varying both the extra-diagonal elements of the matrix A_{trans} within the set of values $\{0.005, 0.01, 0.05, 0.1\}$, and correspondingly the values on its diagonal. Table 4 shows that the larger the probability of transitions, the poorer the performance in terms of DTD and CL indicators. These results are also confirmed by the one-tail Kolmogorov-Smirnov (K-S) tests [34], which checks whether the distributions of the DTD and CL performance indicators obtained with A_{12}=0.01, are similar to the corresponding distributions obtained with A_{12}=0.005 and A_{12}=0.05, respectively. Table 5 shows that there is a strong evidence that the performance indicators related to A_{12}=0.01 are significantly different from those related to 0.05, as witnessed by the small values of the p-value. These results are explained by the fact that frequent transitions from a model to another lead to re-setting the crack length to 0 too often, thus preventing the particles from swapping to the correct model. This suggests that both the probability of

occurrence and the speed of the crack growth must be taken into account when setting the transition matrix values. On the other side, there is not a strong statistical evidence supporting the differences between the performance related to A_{12}=0.01 and to A_{12}=0.005. In this respect, notice that if the transition probability is very small (i.e., A_{12}=0.005), the method of augmenting the state space becomes useless: on average, we have 1 out of 100 particles changing the reference model every two steps. Thus, the method turns out to be not enough reactive to changes in the model.

A_{12}	**0.005**	**0.01**	**0.05**	**0.1**
DTD	20.1	18.6	25.1	38.6
CL	1.27	1.24	1.31	1.54
False Alarms	0%	1%	0%	0%

Table 4 Average Detection Time Delay, Crack Length and Percentage of False Alarms evaluated on a sample of 100 simulated cracks, for different values of the transition probability A_{12}.

A_{12}	**0.005**	**0.05**
p-value($DTD_{0.01}$)	0.161	0.0006
p-value($CL_{0.01}$)	0.134	0.0003

Table 5 One tail K-S tests between the DTD and CL distributions obtained with A_{12}=0.01 and the same distributions obtained with A_{12}=0.005 and A_{12}=0.05 respectively.

With respect to the assessment of the sensitivity of the proposed approach to the measurement error, three performance indicators have been evaluated considering different values of the standard deviation of the measurement noise $\sigma_v \in \left\{\frac{1}{8}, \frac{1}{4}, \frac{1}{2}, 1, 2, 4, 8\right\} \cdot \sigma_{v\,rif}$. This entails that σ_v takes values of different magnitude with respect to the measurement resolution mc: when $\sigma_v = 8 \cdot \sigma_{v\,rif} = 4$, then the precision in the measurement system is very low, whereas it is really high when $\sigma_v = \frac{1}{8} \cdot \sigma_{v\,rif} = \frac{1}{16}$. From Table 6, it emerges that the DTD values of the three methods are similar for small values of σ_v, whereas the IMM method is by far the most accurate when σ_v is comparable with or higher than the measurement resolution mc $(0.5 \leq \sigma_v < 4)$.

Considering, for example, the difference between IMM and MS with $\sigma_\nu = 1$, the K-S test provides a p-value = $6 \cdot 10^{-20}$ confirming the outstanding performance of the IMM approach. On the contrary, when the measurement error is very small ($\sigma_\nu < 0.5$), all the methods are capable of distinguishing the degradation conditions from the normal conditions in a limited time. This result is also confirmed by Table 7. In particular, the considerable worsening of the performance of the method proposed in [10] is due to the need of the MS method of relying on a large window to catch the difference between the two models in correspondence of large values of σ_ν. However, even if w is markedly increased (i.e., w=300), the value of the DTD indicator corresponding to the MS method is still worse than that of IMM (see Fig. 13), as confirmed by a K-S test, whose p-value = $1.4 \cdot 10^{-28}$, and even with higher computational costs (e.g., according to Table 3, the computational time is three times longer, ~95 s / crack).

Finally, Table 8 reports the percentage of false alarms for the same range of σ_ν. This performance indicator is constant for ST, as the value of the standard deviation directly enters the statistical tests, which have the same I type error value α_{ST}. With respect to both the PF-based methods, the false alarm percentage is not null only if the standard deviation takes intermediate values, i.e., when σ_ν takes a value similar to mc. This is due the fact that a smaller σ_ν entails that the observed values of the crack length are similar to their actual values. Thus, the estimation provided by the PF is more accurate. On the other side, the percentage of false alarms in MS decreases in correspondence of larger values of σ_ν, because in this setting MS needs larger windows to get the statistical evidence to state that the difference between the two alternative evolution models is significant. With regards to IMM, larger values of σ_ν lead to a reduction in the probability of giving importance to the particles that are beyond the mc threshold. In details, assume for example that we acquire a measurement at $2\sigma_\nu$ for σ_ν = 1 and 2 (Fig. 14): then, due to

the dynamics of the updating step which is driven by $p(\boldsymbol{y_k}|\boldsymbol{x_k})$, the particles above the mc threshold ($\boldsymbol{x} = 0.5$, in Fig. 14) gain a larger weight when $\sigma_v = 1$ than when $\sigma_v = 2$; thus, the algorithm is more sensitive to false alarms when $\sigma_v = 1$ than when $\sigma_v = 2$.

$\boldsymbol{\sigma_v}$	**0.0675**	**0.125**	**0.25**	**0.5**	**1**	**2**	**4**
ST(DTD)	**3,9**	**4,4**	**10,6**	**44,3**	**107,3**	**183,0**	**301,1**
IMM(DTD)	**1,7**	**3,2**	**7,9**	**19,8**	**50,7**	**110,5**	**198,6**
MS(DTD)	**1,0**	**2,2**	**6,4**	**22,1**	**90,3**	**242,7**	**514,0**

Table 6 Average of the DTD performance indicator for ST, IMM and MS, and for increasing values of the standard deviation of the measurement noise.

$\boldsymbol{\sigma_v}$	**0.0675**	**0.125**	**0.25**	**0.5**	**1**	**2**	**4**
ST(CL)	**1,06**	**1,07**	**1,14**	**1,61**	**2,81**	**4,88**	**9,64**
IMM(CL)	**1,04**	**1,05**	**1,11**	**1,25**	**1,72**	**2,86**	**5,28**
MS(CL)	**1,03**	**1,04**	**1,09**	**1,28**	**2,45**	**6,80**	**24,12**

Table 7 Average of the CL performance indicator for ST, IMM and MS, and for increasing values of the standard deviation of the measurement noise.

$\boldsymbol{\sigma_v}$	**0.0675**	**0.125**	**0.25**	**0.5**	**1**	**2**	**4**
ST False Alarms	**6**	**6**	**6**	**6**	**6**	**6**	**6**
IMM False Alarms	**0**	**0**	**1**	**3**	**3**	**1**	**0**
MS False Alarms	**0**	**4**	**10**	**6**	**0**	**0**	**0**

Table 8 Percentage of false alarms evaluated for different values of the standard deviation of the measurement noise.

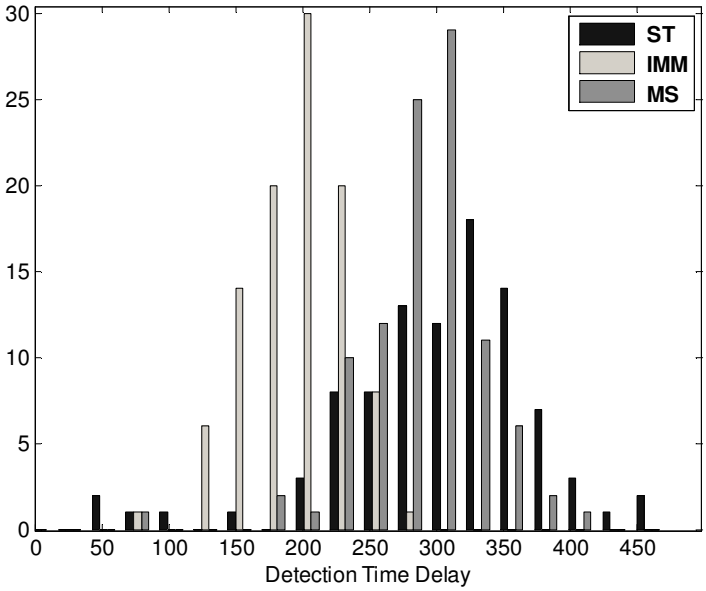


Fig. 13 DTD for the three methods analyzed with σ_ν=4, where MS has been run with $w = 300$.

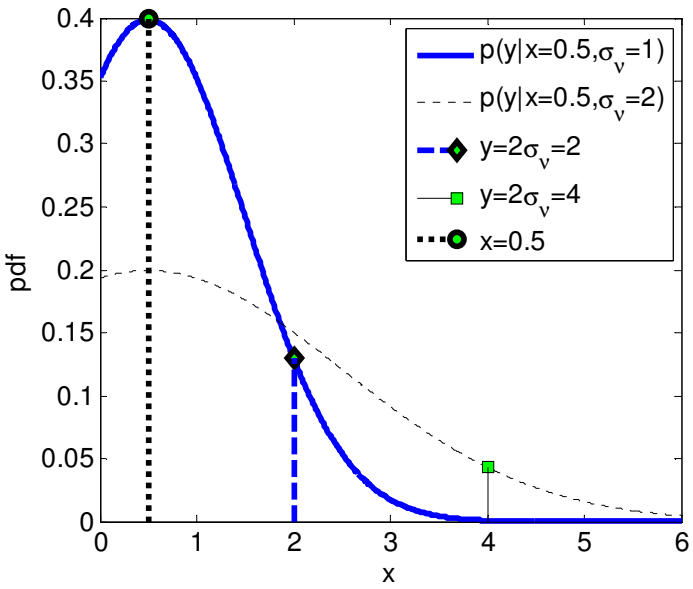


Fig. 14 Updating step when $x_k = 0.5$.

5.2 THREE-MODEL SETTING

The objective of this case study is to evaluate the diagnostic capability of the IMM PF, i.e., the quickness and accuracy in identifying the model that better describes the crack evolution at a

given stage. In this regard, the three-phases model for crack propagation introduced in Section 2 has been considered. The models available are:

1) Normal conditions: during the crack incubation phase, we assume that the crack is not propagating; in this phase, the crack length is modeled as in section 5.1.1:

$$m_n : x_k = \begin{cases} x_{k-1} & if\ x_{k-1} < \epsilon \\ \sim Unif([0, \epsilon)) & otherwise \end{cases} \quad \textbf{(15)}$$

2) Degradation mechanism 1: crack initiation phase, which is modeled by a linear process:

$$m_{d1} : x_k = x_{k-1} + a \cdot e^{\omega_k^1} \quad \textbf{(16)}$$

where $a = 0.003$ is the growth speed parameter and $\omega_k^1 \sim N(-0.625, 1.5)$ models the uncertainty in the speed;

3) Degradation mechanism 2: crack rapid-propagation phase, which is described by the Paris-Erdogan model:

$$m_d : x_k = \begin{cases} x_{k-1} + C \cdot e^{\omega_k^2} \left(\beta \cdot \sqrt{x_{k-1}}\right)^n & if\ x_{k-1} > \epsilon \\ \epsilon & otherwise \end{cases} \quad \textbf{(17)}$$

where the parameters values are the same of those of the two-model system in section 5.1.1.

The measurement system is that in Eq. **(13)**, with the same parameter values.

Notice that the distribution of the noise in the initiating phase is different from that in the rapid-propagation phase. This gives due account to the fact that the crack during the initial degradation is highly influenced by exogenous factors, and it is hardly measurable due to its small length; hence, its uncertainty is expected to be larger.

Fig. 15 reports the simulation of a possible crack growth evolution and an associated possible measurement signal. All the simulated crack growth evolutions start at $T_{Crack} = 400$ units of time and follow the first degradation mechanism according to the model in Eq. **(16)** up to

$T_{PE} = 800$ units of time, when they switch to the second degradation mechanism according to the Paris-Erdogan model in Eq. **(17)**. In this respect, notice that the performance indicators are related to the identification delay time; then, the choice of setting a fixed swap time does not affect the generality of the results.

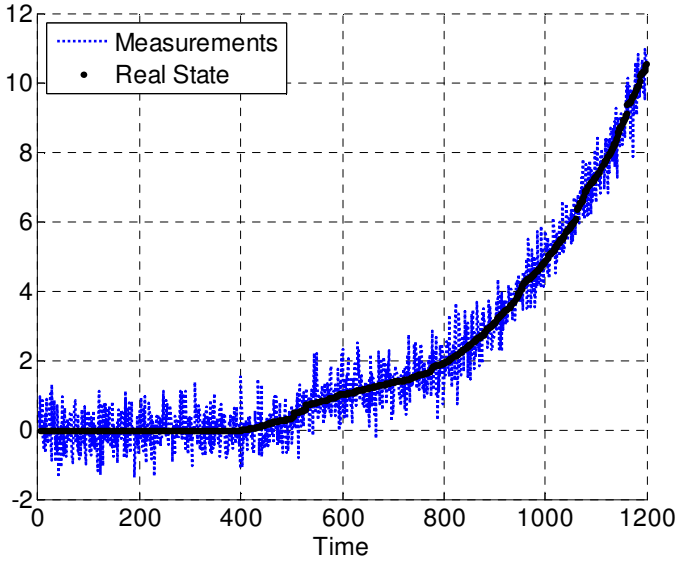


Fig. 15 Crack growth evolution (bold line) and measurements (dot line).

Performances have been evaluated by simulating $N_{Crack} = 500$ crack growth processes, and computing the following performance indicators, which are slightly different from those defined in Section 5.1.3 for the two model setting:

1) *Detection Time Delay (DTD)*, i.e., $DTD = T_{detection} - T_{optimal\,detection}$, where $T_{detection}$ is the time at which the marginalized probability μ_k^{d1} of being in state θ_{d1} (first degradation mechanism) exceeds the threshold μ_T, and $T_{optimal\,detection} = \min_k\{\, k : x_k > mc \,\}$ indicates the time instant at which the crack has reached the mc threshold. DTD is an indicator of the promptness of the method in detecting the incipient degradation.

2) *Transition Time Delay (TTD)*, i.e., $TTD = T_{transition} - T_{optimal\ transition}$, where $T_{transition}$ is the time at which the marginalized probability μ_k^{d2} of being in state θ_{d2} (second degradation mechanism) exceeds the threshold μ_T, and $T_{optimal\ transition} = \min_k\{\, k : \theta_k = \theta_{d2} \,\}$ indicates the time instant at which the crack starts the degradation phase of rapid propagation. TTD is an indicator of the promptness of the method in detecting the second degradation mechanism.

3) *Percentage of False Alarms*, which can concern both the two transitions. According to the former (first degradation mechanism): the number of alarms given when the crack is in the incubation phase (normal conditions), over the number of simulated crack growth processes. According to the latter (second degradation mechanism): the number of second degradation mechanism detected when the crack is in the incubation or in the former degradation phase, over the number of simulated crack growth processes. It is a wide spread index for the robustness of the method.

On the basis of considerations similar to those of the previous cases study, the degradation phase transition probability matrix is set to:

$$A_{trans} = \begin{bmatrix} 0.98 & 0.015 & 0.005 \\ 0.01 & 0.98 & 0.01 \\ 0.005 & 0.005 & 0.99 \end{bmatrix} \quad \textbf{(18)}$$

where we maintain constant the cumulative probability of having a transition from the crack propagation phase to the incubation phase (A_{31} and A_{32}), in order to avoid a too frequent reset of particle crack lengths to 0. On the contrary, we allow particles to jump directly from the incubation to the second degradation mechanism, in order to increase the reactiveness of the filter.

As in the two-model case study, the number of particles is set to $N_S = 100$, whereas the detection threshold is set to $\mu_T = 0.8$, with a number $seq_{detection} = 5$ of consecutive detections required to give the detection alarm.

Fig. 16 shows that the IMM is able to detect the changes in the operational models on the basis of the marginal posterior probability in Eqs. **(8)** and **(10)**, with good filtering performances as confirmed by Fig. 17. Indeed, in the first phase (i.e., $k < T_{crack} = 400$) the marginal probability μ_k^n associated to the incubation model takes by far the highest value; in the second phase (i.e., $T_{crack} < k < T_{trans} = 800$) the probability μ_k^{d1} of the first degradation mechanism takes by far the highest value; whereas, in the last time span the value μ_k^{d2} associated to the second degradation mechanism takes the highest value. Notice that the identification of the transition between incubation and first degradation model (i.e., $m_n \rightarrow m_{d1}$) is more accurate than that between the first and second degradation models (i.e., $m_{d1} \rightarrow m_{d2}$), as it can be seen from the large overlapping in the time span $[\sim 800, \sim 900]$ in Fig. 17, which is indicative of large uncertainty in the variable *H* to be associated to μ_k^H, see Eq. (10). In this respect, Fig. 18 and Fig. 19 show that the distribution of the DTD is centered on a smaller value and presents a sharper shape than that of the distribution of the TTD. This is due to the gradual transition between the degradation models in Eqs. **(16)** and **(17)**, as confirmed by the percentage of false alarms reported in Table 9, which is smaller in the first transition.

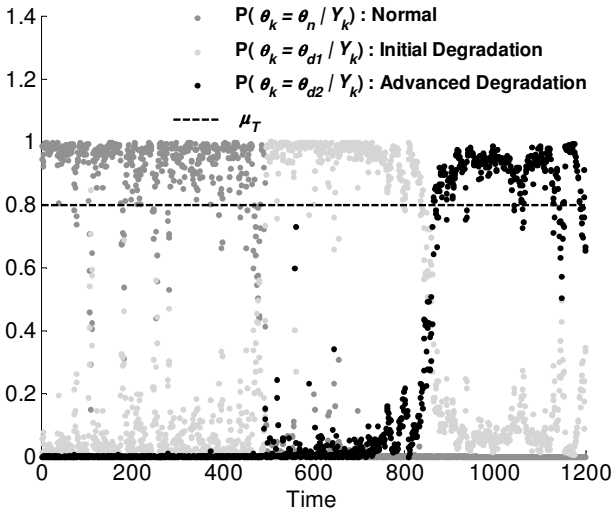


Fig. 16 Marginal posterior probability for every operating models.

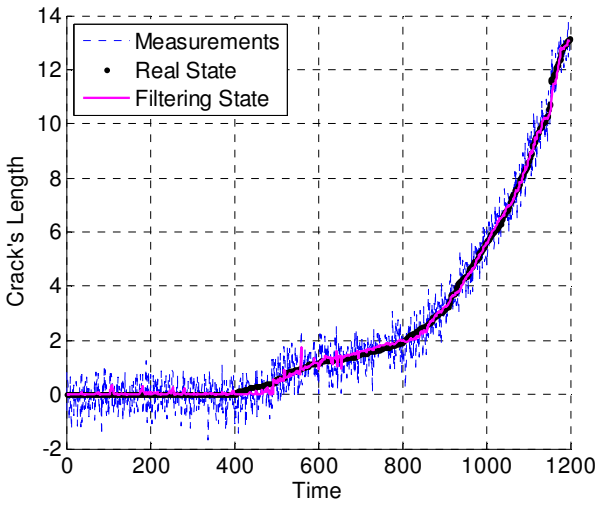


Fig. 17 IMM filtering of the real length of the crack.

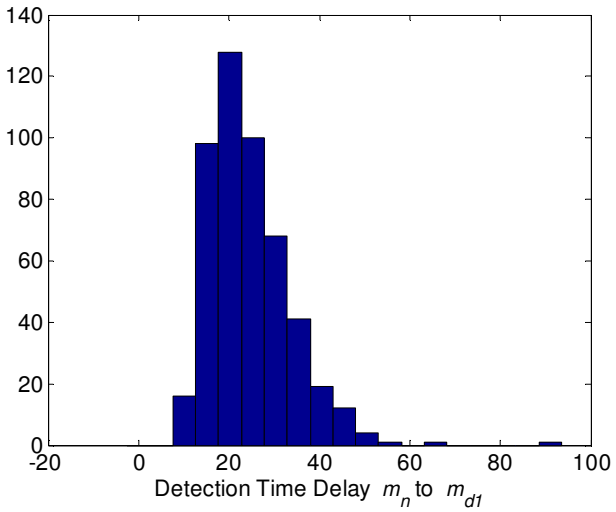


Fig. 18 Histogram of the DTD from the incubation model to the first degradation mechanism.

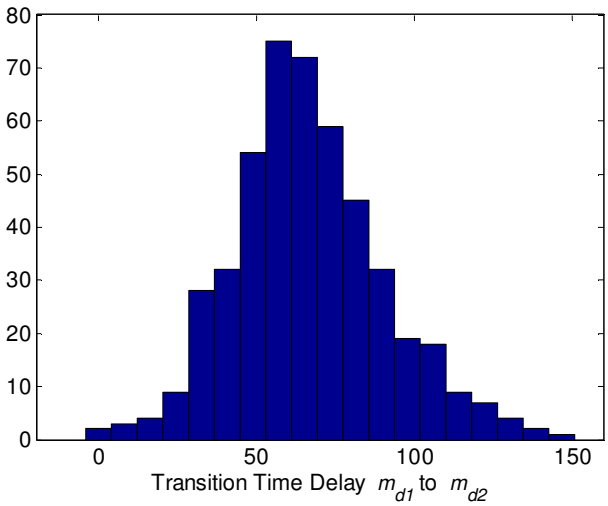


Fig. 19 Histogram of the TTD from the first degradation mechanism to the second degradation mechanism.

Transition	$m_n \rightarrow m_{d1}$	$m_{d1} \rightarrow m_{d2}$
False Alarms	2.2%	5%

Table 9 Percentage of False Alarms evaluated on 500 simulated cracks.

Different choices of μ_T and $seq_{detection}$ entail different performances. Intuitively, small values of $seq_{detection}$ and μ_T make the method sensitive to possible outliers related to measurement noise, as it is confirmed by the high percentage of false alarms, see Fig. 20. On the other side, large values of $seq_{detection}$ and μ_T make the method more conservative, as it is confirmed by the increased delay in DTD and TTD.

Finally, Table 10 and Table 11 report the average of the DDT and TTD for increasing values of $seq_{detection}$ and μ_T, respectively. As expected, the mean values take value in ascending order according to both increasing value of $seq_{detection}$ and μ_T.

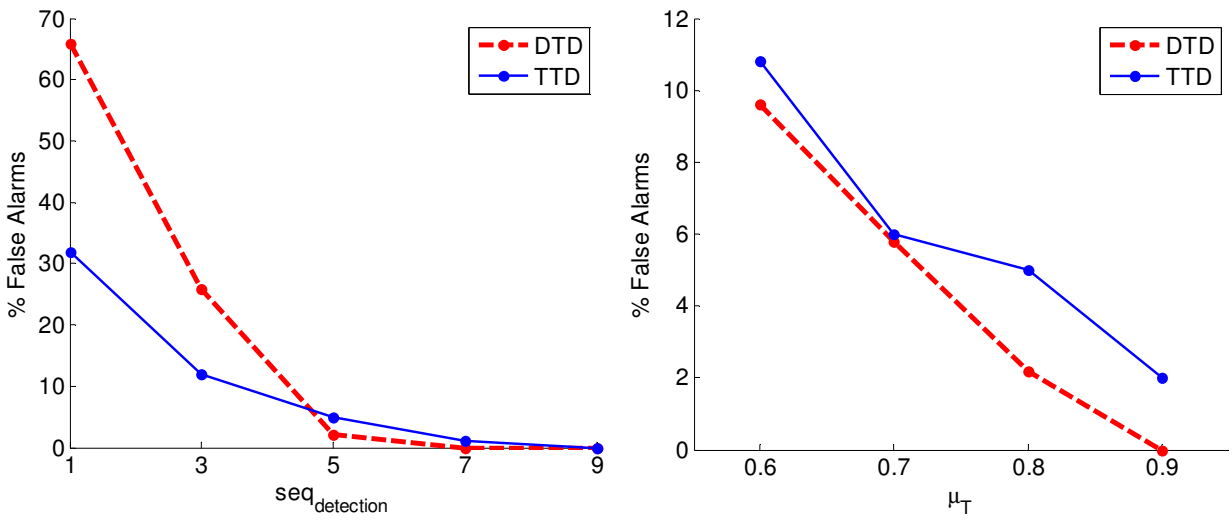


Fig. 20 Percentage of False Alarms: left column sensitivity to $seq_{detection}$; right column sensitivity to μ_T.

$seq_{detection}$	1	3	5	7	9
DTD	**9,6**	**14,7**	**24,4**	**43,1**	**82,4**
TTD	**46,9**	**54,7**	**66,7**	**89,6**	**121,6**

Table 10 Average of DTD and TTD for ascending values of consecutive detection.

μ_T	0.6	0.7	0.8	0.9
DTD	**20,4**	**22,0**	**24,4**	**31,8**
TTD	**53,3**	**58,3**	**66,7**	**96,8**

Table 11 Average of DTD and TTD for ascending values of the detection threshold.

6. CONCLUSIONS

This work has investigated the potential of a PF approach based on an augmented state vector, for fault detection and isolation of nonlinear multi-model gradual degradation processes. By way of a case study concerning crack growth degradation, it has been shown that the proposed approach is capable of performing accurate and prompt detection of the crack occurrence, and of providing robust estimation of the crack length. The computational cost required by the Interacting Multiple Model PF method has resulted one order of magnitude smaller than that of the literature Multiple Swarms PF technique. The diagnostic capability of the method has been confirmed also when the degradation process is modeled as evolving across multiple (three) phases, with smooth transitions from one phase to another.

The performance of the method has been compared to those of an already available PF technique of literature and a statistical sequential test method. It has been shown that the detection performance of the proposed technique is better than those of the other two methods. Furthermore, the introduction of the augmented state which explicitly indicates the process phase allows providing the probability of being in a specific phase, which can be easily used for decision-making. In this respect, future work will focus on the introduction in the model of a risk function, which takes into account the costs associated to false alarms and identification delays. This could give the opportunity of developing a risk-based FDI.

Finally, it is worth noticing that the performance of the proposed method and, more generally, of the PF approach depends on the frequency of measurements. In real applications, it is fundamental to assess whether the frequency of measurements provided by the sensor undermines its applicability. To this aim, future research works will be devoted to perform sensitivity analyses in order to quantify the influence of the measurement frequency on the diagnostic performance. In our work, we have considered the transition probability matrix as

constant and fixed, but it could be useful to introduce the dependencies between the length of the crack and the transition probabilities in order to improve the performance of the method by exploiting new information collected during the evolution of the model. A further aspect to be investigated is how to set the process noise standard deviation, which in the present work has been assumed to be known.

Acknowledgments

The participation of Piero Baraldi to this research is partially supported by the European Union Project INNovation through Human Factors in risk analysis and management (INNHF, www.innhf.eu) funded by the 7th framework program FP7-PEOPLE-2011- Initial Training Network: Marie-Curie Action. The participation of Enrico Zio to this research is partially supported by the China NSFC under grant number 71231001. Also, many thanks go to the reviewers for their constructive comments which have allowed improving the paper.

REFERENCES

[1] Alrowaie F., Gopalunin R.B., Kwok K.E., 2012, "*Fault detection and isolation in stochastic non-linear state-space models using particle filters*", Control Engineering Practice, vol. 20, 1016–1032.

[2] Andrieu C., Djurić P. M., Doucet A., 2001, *"Model selection by MCMC computation",* Signal Processing, vol. 81, No.1, pp. 19-37.

[3] Arulampalam S., Maskell S., Gordon N., Clapp T., 2002, "*A tutorial on particle filters for on-line nonlinear/non-Gaussian Bayesian tracking*", IEEE Transaction on Signal Processing, vol. 50, No. 2, pp. 174-188.

[4] Baraldi P., Mangili F., Zio E., 2012, *"A Kalman filter-based ensemble approach with application to turbine creep prognostics"*, IEEE Transaction on Reliability, vol. 61, No. 4, pp. 966-977.

[5] Basseville M., 1988. "*Detecting Changes in Signals and System – A survey*", Automatica, vol. 24, No. 3, pp. 309-326.

[6] Bishop C., 1995, "*Neural Networks for Pattern Recognition*", Oxford University Press, NY, USA.

[7] Bolotin V.V., Babkin A.A., Belousov I.L., 1998, *"Probabilistic model of early fatigue crack growth",* Probabilistic Engineering Mechanics, vol. 13, No. 3, pp. 227-232

[8] Boursier J.M., Desjardins D. and Vaillant F., 1995, *"The Influence of the strain-rate on the stress corrosion cracking of alloy 600 in high temperature primary water"*, Corrosion Science, vol. 37, No. 3, pp. 493-508.

[9] Cadini F., Zio E., Avram D., 2009, "*Monte Carlo-based filtering for fatigue crack growth estimation*", Probabilistic Engineering Mechanics, vol. 24, No 3, pp. 367-373.

[10] Cadini F., Zio E., Giovanni Peloni, 2012, "*Particle Filtering for the Detection of Fault Onset Time in Hybrid Dynamic Systems With Autonomous Transitions*", IEEE Transaction on reliability, vol. 61, No. 1, pp. 130-139.

[11] Castanier B., C.Bérenguer and Grall A., 2003, *"A sequential condition-based repair/replacement policy with non-periodic inspections for a system subject to continuous wear"*, Applied Stochastic Models in Business and Industry, vol. 19, No 4, pp. 327-347.

[12] Ding S. X., 2008, "*Model-based fault diagnosis techniques*", vol. 2013, Springer, Berlin.

[13] DOT/FAA/AR, 2005, *"Fatigue Crack Growth Database for Damage Tolerance Analysis*", Final Report, Federal Aviation Administration, Washington, D.C..

[14] Doucet A. N., Johansen A. M., 2008, "*A Tutorial on particle filtering and smoothing: Fifteen years later*".

[15] Doucet. A., N. De Freitas and N.J. Gordon, 2001, *"An introduction to Sequential Monte Carlo Methods"* in SMC in Practice, Springer-Verlag, New York.

[16] Gertler J., 1997, *"Fault detection and isolation using parity relations"*, Control Eng. Practice, vol. 5, No. 5, pp. 653-661.

[17] Grall, A., Blain, C., Barros, A., Lefebvre, Y., F.Billy, 2007, *"Modeling of Stress Corrorsion Cracking with Periodic Inspection",* Proceeding of the 32nd ESReDA Seminar, Alghero, Italy Maintenance Modeling and Application, vol. 1, pp. 253-260.

[18] Green P. J., 1995, *"Reversible jump Markov chain Monte Carlo computation and Bayesian model determination"*, Biometrika, vol. 82, pp.711-732.

[19] Henk A., Blom P., Bar-shalom Y., 1988, "*The interacting multiple model algorithm for system with Markovian switching coefficients*", IEEE Transactions on Automatic Control, vol. 33, No. 8.

[20] Hsu C., Chang C., Lin C., 2003, *"A Practical Guide to Support Vector Classification",* Department of Computer Science and Information Engineering, National Taiwan University, Taipei.

[21] Hu Y., Baraldi P., Di Maio F., Zio E., 2015, *"A particle filtering and kernel smoothing-based approach for new design component prognostics*", Reliability Engineering & System Safety, vol. 134, pp. 19-31.

[22] Hwang I., Kim S., Kim Y., Seah C.E., 2010, *"A Survey of Fault Detection, Isolation, and Reconfiguration Methods",* Control Systems Technology, IEEE Transactions on, vol.18, No.3, pp. 636-653.

[23] Isermann R., 2005, *"Model-based fault-detection and diagnosis – status and applications"*, Annual Reviews in Control, vol. 29, No. 1, pp. 71-85.

[24] Jardine A., Lin D., Banjevic D., 2006, "*A review on machinery diagnostics and prognostics implementing condition based maintenance"*, Mechanical Systems and Signal Processing, vol. 20, No. 7, pp. 1483–1510.

[25] Jarrell D.B., Sisk D.R., Bond, L.J., 2004, *"Prognostics and Condition-Based Maintenance: A New Approach to Precursive Metrics"*, Nuclear Technology, vol. 145, pp. 275-286.

[26] Johnson, Richard Arnold, and Dean W. Wichern. *"Applied multivariate statistical analysis."* Vol. 4. Englewood Cliffs, NJ: Prentice hall, 1992.

[27] Julier, S. J. and Uhlmann, J. K., 1997, *"A new extension of the Kalman filter to nonlinear systems"*, SPIE Aerospace Symposium.

[28] Kadirkamanathan V., Li P., 2001, *"Particle Filtering based likelihood ration approach to fault diagnosis in nonlinear stochastic system"*, IEEE Transaction on Systems, Man and Cybernetics – part C: Application and Reviews, vol. 31, No. 3,pp. 337-343.

[29] Kadirkamanathan V., Li P., 2004, "*Fault detection and isolation in non-linear stochastic systems–A combined adaptive Monte Carlo filtering and likelihood ratio approach*", International Journal of Systems Science, vol. 77, No. 12, pp. 1101–1114.

[30] Kozin, F., and J. L. Bogdanoff. "Probabilistic models of fatigue crack growth: results and speculations." *Nuclear engineering and design* 115.1 (1989): 143-171.

[31] Li X.-R., Bar-Shalom Y., 1996, *"Multiple-model estimation with variable structure"*, Automatic Control, IEEE Transactions on, vol. 41, No. 4, pp. 478-93.

[32] Liu J.S., Chen R., 1998, "*Sequential Monte Carlo method for dynamic system*", Journal of the America Statistic Association, vol. 93, No. 443.

[33] Liu W., Principe J., Haykin S., 2010, *"Kernel Adaptive Filtering: A Comprehensive Introduction*", John Wiley, Hoboken, New Jersey, USA.

[34] Massey F. J., 1951, "*The Kolmogorov-Smirnov Test for Goodness of Fit."* Journal of the American Statistical Association, vol. 46, No. 253, pp. 68–78.

[35] Mehra, M. Rago, C. and Seereeram, S., 1998, *"Autonomous failure detection, identification and fault-tolerant estimation with aerospace applications"*, in Proceedings of IEEE Aerospace Conference, vol. 2, pp.133-138.

[36] Mehra, M., Seereeram, S., Bayard, D. and Hadaegh, F., 1995, *"Adaptive Kalman filtering, failure detection and identification for spacecraft attitude estimation"*, in Proceedings of the 4th IEEE Conference on Control Applications, pp.176-181.

[37] Myötyri E., Pulkkinen U., Simola K., 2006, *"Application of stochastic filtering for lifetime prediction"*, Reliability Engineering & System Safety, vol. 91, No. 2, pp. 200-208.

[38] Orchard M., Vachtsevanos G., 2009, *"A particle-filtering approach for on-line fault diagnosis and failure prognosis",* Transactions of the Institute of Measurement and Control, vol. 31, No. ¾, pp. 221–246.

[39] Papoulis A., Pillai U., 2002, *"Probability, Random Variables, and Stochastic Processes"*, Mc Graw-Hill, 4th Edition.

[40] Paris P., Erdogan F., 1963, *"A Critical Analysis of Crack Propagation Laws"*, Journal of Basic Engineering, vol. 85, No. 4, pp. 528-533.

[41] Provan J. W., 1987, *"Probabilistic fracture mechanics and reliability"* Martinus Nijhoff Publishers, P. O. Box 163, 3300 AD Dordrecht, The Netherlands.

[42] Rasmussen C., Williams C., 2006, *"Gaussian Processes for Machine Learning*", MIT Press, Cambridge, MA, USA.

[43] Schijve J., 2003, *"Fatigue of structures and material in 20th century and the state of art"*, International Journal of Fatigue, vol. 25, pp. 679-702.

[44] Thrun S., Langford J., Verma V., 2001, *"Risk sensitive particle filters",* Advances in Neural Information Processing Systems, vol. 14.

[45] Venkatasubramanian V., R. Rengaswamy, K. Yin, S. N. Kavuri, 2003, "*A review of process fault detection and diagnosis Part I: Quantitative model-based methods*", Computers and Chemical Engineering, vol. 27, pp. 293-311.

[46] Venkatasubramanian V., R. Rengaswamy, S. N. Kavuri, 2003, "*A review of process fault detection and diagnosis Part II: Qualitative models and search strategies*", Computers and Chemical Engineering, vol. 27, pp. 313-326.

[47] Venkatasubramanian V., R. Rengaswamy, S. N. Kavuri, K. Yin, 2003, "*A review of process fault detection and diagnosis Part III: Process history based methods*", Computers and Chemical Engineering, vol. 27,pp. 327-346.

[48] Wang X., Syrmos V. L., 2008, "*Interacting Multiple Particle Filters For Fault Diagnosis of Non-linear Stochastic Systems*", American Control Conference, Seattle, USA.

[49] Willsky A.S. et al., 1980, "*Dynamic model-based techniques for the detection of incidents on freeways*", IEEE Trans. Automat. Contr., vol. AC-25.

[50] Worden K., Staszewski W., Hensman J., 2011, *"Natural computing for mechanical systems research: a tutorial overview"*, Mechanical Systems and Signal Processing, vol. 25, No. 1,pp. 4–111.

[51] Zhang B., Sconyers C., Byington C., Patrick R., Orchard M., Vachtsevanos G., 2008, *"Anomaly detection: a robust approach to detection of unanticipated faults"*, International conference on prognostics and health management.

[52] Zhang B., Sconyers C., Byington C., Patrick R., Orchard M., Vachtsevanos G., 2011, *"A probabilistic fault detection approach: application to bearing fault detection"*, IEEE transaction on industrial electronics, vol. 58, No. 5., 2011-2018.

[53] Zio E., Zoia A., 2009, *"Parameter Identification in Degradation Modeling by Reversible-Jump Markov Chain Monte Carlo",* Reliability, IEEE Transactions on, vol.58, No.1, pp.123-131.

[54] Zio E., 2013, *"Diagnostic and Prognostic of Engineering System: Methods and Techniques"*, IGI Global, pp. 333-356.